

# The wettability of titanium diboride by molten aluminum drops

D. A. WEIRAUCH, JR.\* , W. J. KRAFICK  
Alcoa Technical Center, Alcoa Center, Pennsylvania, 15069, USA  
E-mail: douglas.weirauch@alcoa.com

G. ACKART, P. D. OWNBY  
Ceramic Engineering Department, University of Missouri, Rolla, Missouri, 65401, USA

Titanium diboride is widely accepted to be completely wet by liquid aluminum, yet few published wetting studies demonstrate this behavior, and reported contact angles vary widely. Sessile drop substrates from four different sources were selected and their microstructures and chemistries characterized. The results of sessile drop experiments using four techniques to modify oxide film behavior were compared. The Al-TiB<sub>2</sub> interfaces were examined in metallographic sections or after chemical removal of the Al drop. Al wets a material containing 5.5 wt% Ni in vacuum experiments before the hold temperature of 1025°C is reached. The other TiB<sub>2</sub> substrates are completely wet by Al at 1025°C, but only after prolonged holds under vacuum. Elimination of boron oxide from the TiB<sub>2</sub> surface leads to a spreading condition. The role of the substrate microstructure (porosity, grain size, roughness, and carbon content) in altering the wetting kinetics is discussed.

© 2005 Springer Science + Business Media, Inc.

## 1. Introduction

That TiB<sub>2</sub> is strongly wetted by Al is often reiterated in technical papers dealing with processes involving liquid Al [1, 2]. In actuality there have been very few published studies of the wettability of TiB<sub>2</sub> that provide sufficient technical detail to confirm this statement. The most widely-cited study is that of Rhee who recorded a 55° contact angle for high-purity Al on hot-pressed TiB<sub>2</sub> of 98% theoretical density at 840°C in a vacuum of better than  $2.7 \times 10^{-5}$  Pa [3]. The results of subsequent studies differed widely with no convergence of contact angle data above the well known Al wetting onset temperature of 900–1000°C [3, 5–9]. Furthermore, with the exception of a vapor deposited TiB<sub>2</sub> coating on sapphire [6], none of these studies report perfect wetting (spreading with a contact angle approaching zero) over the temperature range covered. At the first high-temperature capillarity conference, the wetting of dense, hot isostatically-pressed TiB<sub>2</sub> substrates was complemented with detailed analyses of the interfacial chemistry and microstructure [8]. The terminal contact angles attained in a graphite-lined furnace after holds of 8–15 h in a vacuum of approx.  $10^{-3}$  Pa were 10–20 degrees at 990°C. Slow wetting kinetics were attributed to the removal of oxide films from both the aluminum drop and the TiB<sub>2</sub>. It is not readily apparent how much of the difference in contact angle results compared to earlier studies is due to differences in the solid substrates and how much is due to the influence of technique differences on oxide film behavior.

In this study, the wetting of a set of TiB<sub>2</sub> substrates possessing distinctly different microstructures and chemistries by high-purity Al (99.8% or better) is assessed. Several experimental approaches that altered the behaviour of the oxide films formed on Al and TiB<sub>2</sub> during the course of the experiments were employed. These included the use of low-oxygen mixed gas buffer atmospheres, vacuum, Zr-gettered argon, and a molten salt cover.

## 2. Experimental approach

Four different types of TiB<sub>2</sub> were used as substrates in the wetting studies:

- A. better than 99% purity if the 1–2 wt% carbon is excluded,
- B. better than 98% purity with C, W, Fe, and Co the major impurities,
- C. better than 98% purity with C, and Cl the major impurities,
- D. better than 91% purity with 5.5 wt% Ni and C, W, Al, Fe, Cr, and Mo as impurities.

Glow-discharge mass spectrometry was used to quantify impurity levels. Types B-D contain 0.25–1 wt% oxygen, while that in type A is negligible. Elements are present in the samples as impurities in the starting powders, picked up during processing, or intentionally added to control densification and grain growth during

\* Author to whom all correspondence should be addressed.

TABLE I Physical properties of the TiB<sub>2</sub> samples of this study

Sample	Density (g/cm <sup>3</sup> )	Theoretical density (%)	Roughness As-Tested Ra, microns
Type A	4.38	97.2	1.9 and 0.08
Type B	4.49	99.7	2.7 and 0.08
Type C	3.11	69.2	5.7
Type D	4.44	98.6	0.2

Theoretical density of titanium diboride = 4.5 g/cm<sup>3</sup>.

pressure-less sintering [10]. The 5.5 wt% Ni in the type D material and the 1–2 wt% C in the type A are noteworthy. The latter stems from the paraffin wax binder used to produce this material [11]. Key physical properties of the TiB<sub>2</sub> types are listed in Table I.

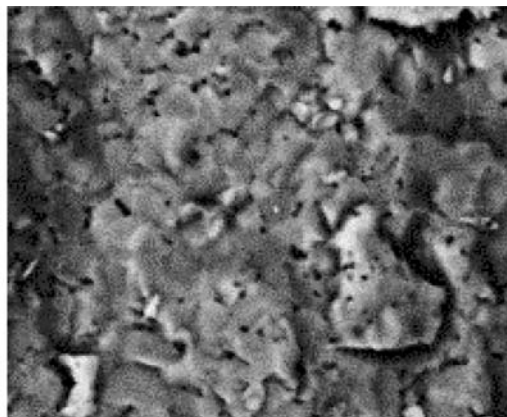
Density was measured by the Archimedes technique and the surface roughness using high resolution optical profilometry. The SEM images of fracture surfaces of the four TiB<sub>2</sub> samples shown in Fig. 1 emphasize that the type C material has a very open and porous structure (approx. 28% open porosity), while the others are very dense with low porosity. The difference in TiB<sub>2</sub> grain size is also apparent with the type A being finest.

Samples were tested with either the as-cut roughness stemming from an EDM wire cutting process

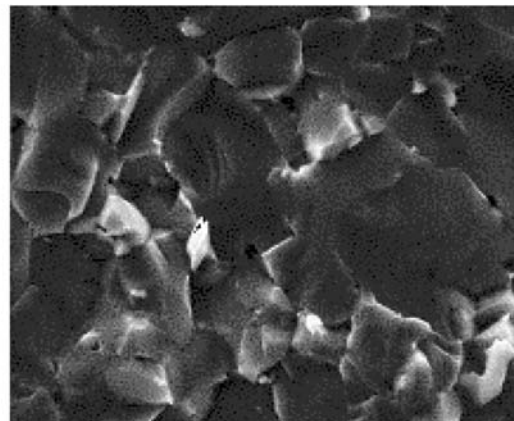
(Table I) or polished to a 1 micron diamond finish ( $R_a = 0.08 \mu\text{m}$ ).

The first type of experiment placed the liquid Al drop on the TiB<sub>2</sub> substrates at high temperature in a controlled atmosphere using the doser technique described previously [12]. This approach allowed the substrate to come into equilibrium with the reducing gas stream at temperature prior to drop placement. The oxygen content of the ultra high purity hydrogen atmosphere was held low enough to prevent TiB<sub>2</sub> oxidation, and held as low as possible as measured with a solid electrolyte to limit the rate of oxidation of the liquid Al drop. The combination of 5N hydrogen (<1 ppm O<sub>2</sub> and <2 ppm H<sub>2</sub>O) with a molecular filter resulted in measured pO<sub>2</sub> levels in the 10<sup>-19</sup> to 10<sup>-24</sup> atm. range at 1025°C (the approx. Al/Al<sub>2</sub>O<sub>3</sub> equilibrium value is pO<sub>2</sub> = 10<sup>-34</sup> atm). In order to remove the influence of gasses desorbed from the cooler ends of the furnace during heat-up, a rough vacuum of approximately 20–40 torr was maintained with a trickle of ultra high purity hydrogen.

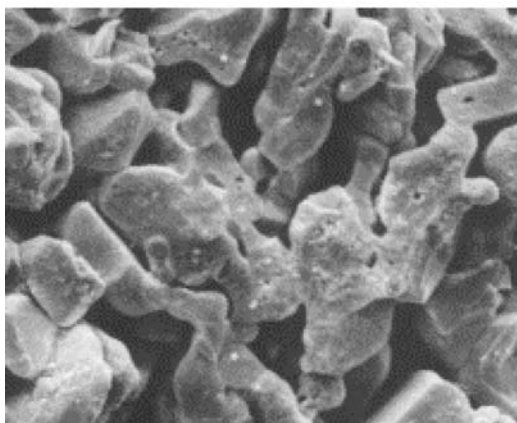
A graphite-lined vacuum furnace was used to form the 0.08–0.10 g drop of liquid Al *in situ* during the 10°C/min ramp to the experimental temperature in a second set of wetting experiments. The solid 6N aluminum was cleaned by sequential 10 min. exposures to a NaOH solution, deionized water, and ethanol and



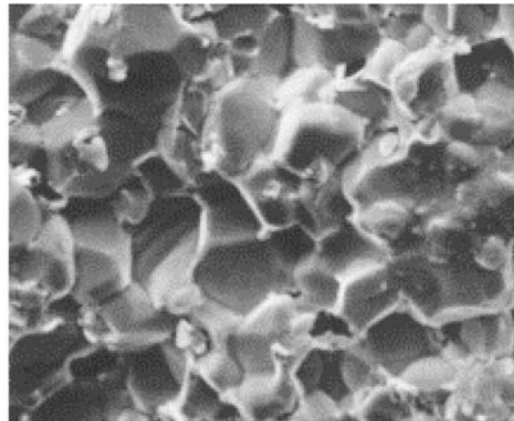
(a) Type A TiB<sub>2</sub>



(b) Type B TiB<sub>2</sub>



(c) Type C TiB<sub>2</sub>



(d) Type D TiB<sub>2</sub>

20 μm

Figure 1 Fracture surfaces of the TiB<sub>2</sub> test samples.

dried under a heat lamp. TiB<sub>2</sub> substrates were cleaned with ethanol only. A vacuum of better than 10<sup>-4</sup> torr (1.3 × 10<sup>-2</sup> Pa) was attained during the hold at the test temperature. The contact angle was measured directly using a telegoniometer [13]. It is well established that a variety of experimental details may influence aluminum wetting results [2]. While this behavior is understood in the context of oxide film effects and intrinsic wetting behavior for some substrates such as single crystal alumina [2, 4, 13] and graphite [2, 14] this is not the case for TiB<sub>2</sub>. These two substrates were therefore included as reference materials in the current study to interpret aluminum and TiB<sub>2</sub> substrate oxide effects in the carbon furnace experiments.

A third experimental approach used in this study involves the formation of an Al drop on the sample substrate in a closed Zr crucible at 1 atm inert gas pressure [15]. This technique was used previously to form oxide-free interfaces yielding the intrinsic contact angle between Al and single crystal aluminum oxide at temperatures above 760°C [16]. The disadvantage of this approach is that it precludes direct observation of the sessile drop at temperature, and some shape distortion due to cooling to room temperature is expected. Experiments using 0.08–0.10 g Al drops were conducted at 760 and 960°C.

A final series of experiments were conducted beneath a cryolitic salt cover. Cryolitic salts have high solubilities of the oxides of Al, B, and Ti [17]. This property can be used to form oxide-free interfaces between Al and TiB<sub>2</sub>, but the effect of the salt on interfacial energies must also be taken into account when interpreting the contact angle. A few experiments were conducted under a molten salt cover to assess the effect of the salt on substrate wetting behavior. In these experiments dried O<sub>2</sub>-free argon was passed over the surface of a Hall Cell salt bath (NaF:AlF<sub>3</sub> = 1.13 by weight, Al<sub>2</sub>O<sub>3</sub> = 2.7 wt%, CaF<sub>2</sub> = 5.9 wt%) at a flow rate of 0.75 cc/min. The 55 g salt bath was contained in either an alumina or graphite crucible with the TiB<sub>2</sub> substrate at its bottom. After the bath had been held for 1 h at 960°C, a 1.0 g piece of Al was dropped onto the substrate. The crucible was removed from the furnace after the desired hold time. Loose salt was mechanically removed from the sessile drop sample and the wetting condition of the substrate was observed.

### 3. Results and discussion

#### 3.1. Low oxygen hydrogen in a rough vacuum

Under these conditions only the type D material exhibited spreading at 1025°C. The other substrates required temperatures higher than 1300°C to achieve a spreading condition. The measured 10<sup>-15</sup> to 10<sup>-20</sup> atm range of the oxygen partial pressures of the furnace atmosphere approaches the equilibrium pO<sub>2</sub> of B/B<sub>2</sub>O<sub>3</sub> at 1300°C (10<sup>-20</sup> atm). While this suggests that the slow wetting kinetics are controlled by reaction with a B<sub>2</sub>O<sub>3</sub> layer on the TiB<sub>2</sub> surface, no characterization of the oxide layers that formed on these materials was conducted.

#### 3.2. Vacuum experiments in graphite-lined furnace

Initial vacuum wetting experiments were conducted at 1025°C in a graphite-lined furnace used as-cut rough TiB<sub>2</sub> surfaces. The observed contact angle changes were a consequence of physical wetting phenomena, chemical reactions and in some cases substrate penetration. Consequently they couldn't be properly interpreted without post-test examination of samples in metallographic section. The apparent contact angle of Al on the type D substrate fell to 15 degrees before the hold temperature of 1025°C was reached. The sectioned sample revealed that the Ni of the substrate reacted with Al and expanded the substrate so that the final apparent contact angle was actually the angle formed on the substrate by the reaction product layer. Similar intense reaction has been reported elsewhere when Ni-TiB<sub>2</sub> composites are exposed to molten Al [18]. The apparent contact angle fell to 0° after a 45 min hold on the type C substrate at 1025°C. The porous type C substrate was penetrated by aluminum so that the observed contact angle changes resulted from a combination of wetting, spreading, and penetration phenomena. Al penetrated into some pores while others remained unfilled. When viewed in metallographic cross section, the type A substrate showed little evidence of chemical reaction or substrate penetration after a 2 h hold at 1025°C. A few Al<sub>4</sub>C<sub>3</sub> particles were observed in cross section in the Al near the Al/TiB<sub>2</sub> interface. The apparent contact angle fell below 10° in the sessile drop experiments held for more than 18 hrs using this substrate. When the samples were extracted from the furnace, it was observed that a thin layer of Al that could not be resolved in the telegoniometer had spread along the substrate surface (Fig. 2c and d).

This secondary spreading halo indicates that the contact angle was low enough to allow spreading along surface capillary channels on the rough surface [2, 19]. Grains of a titanium aluminide presumed to have formed during cooling were observed in cross section in the secondary spreading halo formed on the rough Type B substrate.

The dense type A & B substrates were both polished to a 1micron diamond finish for comparison to wetting on the rough EDM wire-cut surfaces. Single crystal alumina and graphite were used as reference materials since their intrinsic wetting is well understood [2, 4], and experiments in a carbon vacuum furnace were described previously [13, 14]. The wetting kinetics on type A polished surfaces are presented in Fig. 3.

The contact angle of Al on single crystal alumina reached its stable intrinsic value of approx. 80° in 0.1 h and represents the end of the first stage wetting where the aluminum oxide film is removed from the Al sessile drop [4]. Mass loss does not appear to be significant for the first few hours of the experiment. With continued hold in vacuum the contact angle falls to 52°, and several ridges were etched into the single crystal alumina surface when observed after cooling to room temperature. Under conditions of more rapid mass loss (higher temperature under vacuum or better vacuum), Al drops on single crystal alumina have

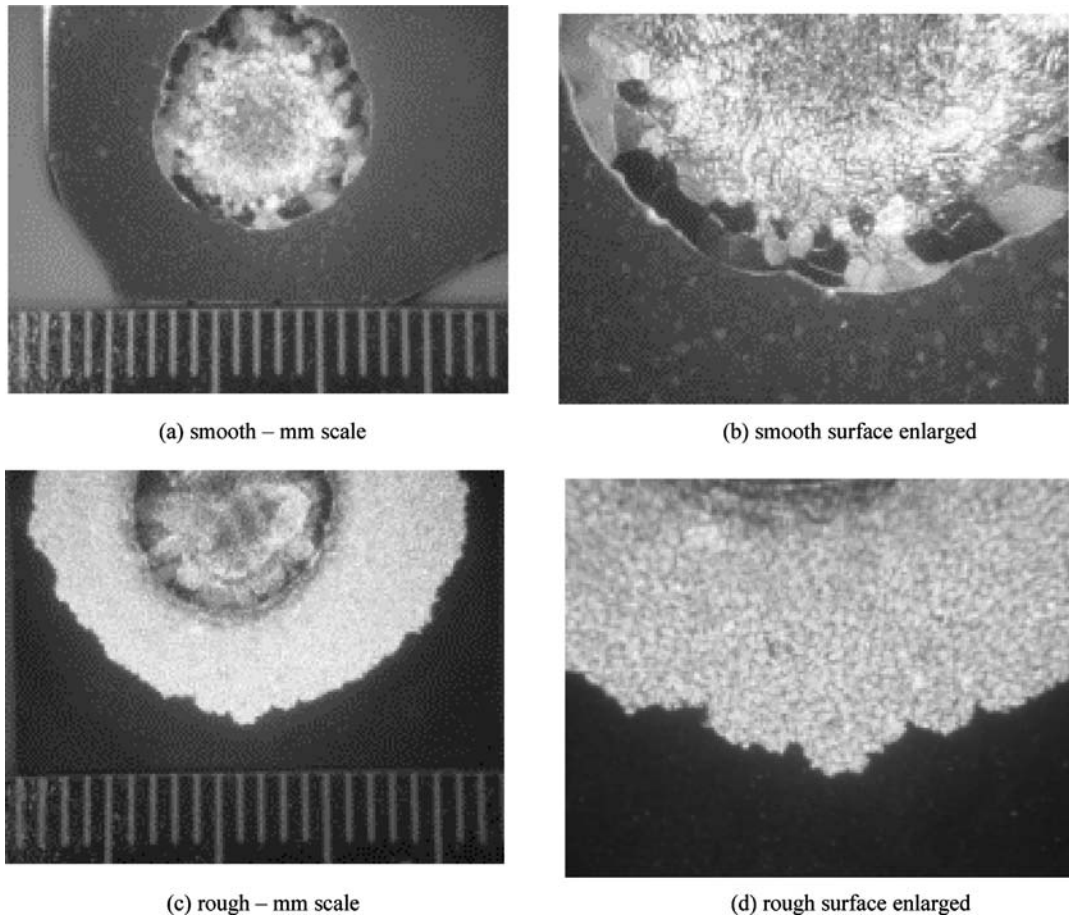


Figure 2 Al spreading fronts on smooth and rough type A TiB<sub>2</sub>.

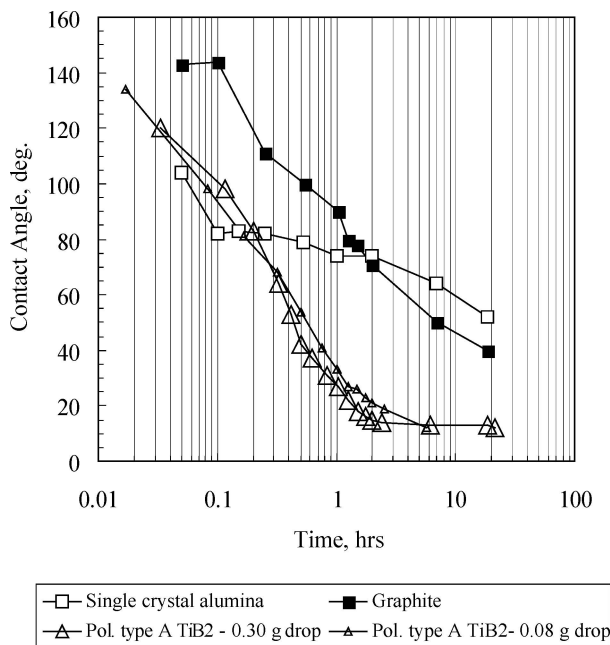


Figure 3 Comparison of TiB<sub>2</sub> wetting under vacuum at 1025°C to that of single crystal alumina and graphite.

been observed to oscillate between these two values as a consequence of the combined evaporation and substrate reaction [20]. The wetting of graphite is slower and it takes 2 h for the 50–70 degree characteristic contact angle [2] to be reached. The rate of TiB<sub>2</sub> wetting is comparable for Al drops of two sizes (0.08 and 0.30 g)

to that on single crystal alumina but continues beyond the intrinsic wetting point for single crystal alumina with continued reaction between aluminum and the surface oxides of the TiB<sub>2</sub>. There is an apparent slowing in contact angle kinetics near the end of the TiB<sub>2</sub> wetting experiment. This is ascribed to a reduction in driving force as the contact angle approaches the intrinsic level of approx. 9–12° for this material containing a few percent carbon. The higher final contact angle on the type A (carbon containing) TiB<sub>2</sub> compared to the near-zero angle reached on the type B material is consistent with observations on the wetting TiB<sub>2</sub>-C composites [21].

The results for both polished and unpolished types A & B TiB<sub>2</sub> in a carbon vacuum furnace are compared to those of Bardal *et al.* [8] who used a similar technique in Fig. 4. These literature experiments were conducted at 990°C, in a better vacuum, but the drop volume was not specified. Despite this, their wetting kinetics following the Al deoxidation stage are very close to those observed for the polished TiB<sub>2</sub> surfaces of this study. They observed non-zero terminal contact angles but their impurity levels were not recorded in the paper. Bardal *et al.* [8] attributed slow linear spreading kinetics for Al on hot-isostatically pressed TiB<sub>2</sub> to the removal of oxide barriers from both the liquid Al drop and the TiB<sub>2</sub> substrate. The rate of spreading on graphite during this stage is similar to that on the rough TiB<sub>2</sub> surface (Figs 3 and 4). The linear spreading rate observed on type A TiB<sub>2</sub> is greatly accelerated by polishing. Landry and Eustathopoulos also observed a deceleration of the

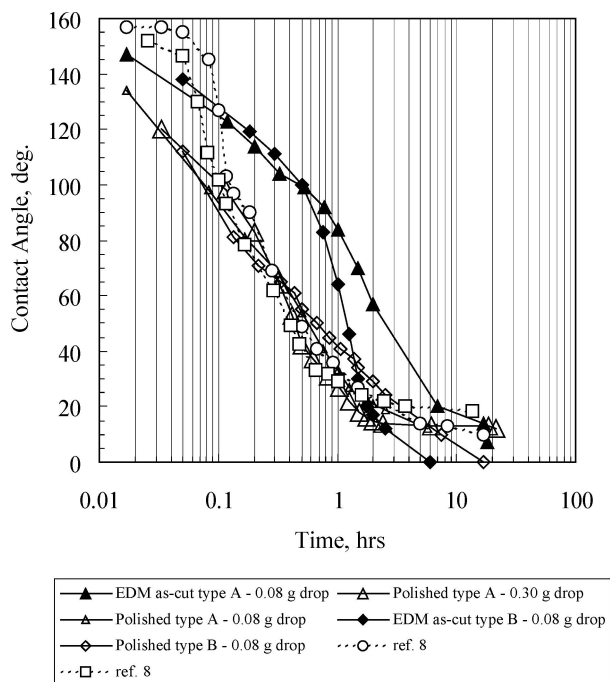


Figure 4 The wetting kinetics of dense, high purity  $\text{TiB}_2$  by Al in a carbon vacuum furnace.

spreading rate following the linear stage [22]. They attributed this process to a decrease in the driving force as the contact angle approached its final value on the reacted substrate, as well as to asperity pinning of the triple line on the roughened surface formed by reaction. In the present study we observed a secondary spreading halo on the rough  $\text{TiB}_2$  surfaces (Fig. 2). The irregularity of the triple line is more pronounced with higher roughness, but there appears to be at least two scales of the triple line distortion. Complete wetting was attained on the polished type B substrate and the irregularity of the spreading front was even more exaggerated. Removal of the Al drop from the type B substrate using a NaOH solution revealed only minor amounts of  $\text{Al}_4\text{C}_3$  and an Al-Ti intermetallic phase. These were presumed to grow from a saturated interface during cooling and should not have been a factor in the distortion of the triple line. More work is required to establish whether the different impurity concentrations, microstructures, or roughness of the materials control the pinning of the triple line as it advances.

### 3.3. 1 atm Zr-gettered argon

A contact angle of  $35^\circ \pm 3$  after a 72 h hold at  $760^\circ\text{C}$  and a similar contact angle of  $40^\circ \pm 3$  after an 18 h hold at  $1025^\circ\text{C}$  was observed on the type A  $\text{TiB}_2$ . This is considerably higher than the  $9\text{--}12^\circ$  contact angle after the same hold time in vacuum at  $1025^\circ\text{C}$ . The difference is attributed to a slower oxide film removal rate from the  $\text{TiB}_2$  surface at 1 atm. pressure. Koh *et al.* studied the oxidation behavior of  $\text{TiB}_2$  at elevated temperatures [23]. Below  $1000^\circ\text{C}$  an outer liquid  $\text{B}_2\text{O}_3$  layer was formed on top of an inner  $\text{TiO}_2$  layer. At higher temperatures, the  $\text{B}_2\text{O}_3$  vaporized and only a  $\text{TiO}_2$  layer was left behind. A sample of  $\text{TiB}_2$  exposed to oxidizing conditions at  $1000^\circ\text{C}$  revealed an increase in the

relative intensity of XRD peaks for  $\text{B}_2\text{O}_3$  up to 2 h followed by a decline and complete disappearance of the  $\text{B}_2\text{O}_3$  after 10 h. This is in remarkably close agreement with the time required in the present study for Al to reach a spreading condition. It may be that  $\text{B}_2\text{O}_3$  removal controls the  $\text{TiB}_2$  wetting kinetics in the present study. More work is required to characterize changes in the oxide films on  $\text{TiB}_2$  occurring under wetting furnace conditions.

### 3.4. Liquid salt cover at 1 atm

The kinetics of wetting  $\text{TiB}_2$  by liquid Al are greatly accelerated under a cryolitic salt cover. A spreading condition was observed in this study after a 5 min hold at  $960^\circ\text{C}$  under the Hall Cell bath, and it may have been achieved at shorter times. Watson and Toguri used radiographic techniques to directly observe the Al spreading kinetics on hot-pressed  $\text{TiB}_2$  under a cryolitic melt cover [24]. They reported a spreading condition within a few seconds at  $980^\circ\text{C}$ . They also observed that the spreading kinetics decreased as the carbon content of  $\text{TiB}_2/\text{C}$  composites increased. In salt cover experiments the Al/vapor interface is replaced by the Al/salt interface altering the driving force for spreading [25]:

$$F = \gamma_{lv}(\cos \theta_{\text{equil}} - \cos \theta_t) \quad (1)$$

The surface tension of Al is 786 dyn/cm [26] and the Al-salt interfacial energy is 525 dyn/cm at  $960^\circ\text{C}$  [27]. By this line of thinking the driving force for spreading would be lower under the salt cover so that the removal of oxide films is the more likely explanation.

## 4. Conclusions

1. A wide range of liquid Al wetting, spreading, and  $\text{TiB}_2$  penetration behavior was observed for the four substrates in  $1025^\circ\text{C}$  carbon vacuum furnace experiments. The dense, high-purity type B  $\text{TiB}_2$  was strongly wet by Al and achieved a contact angle =  $0^\circ$  on a polished surface within 17 h at  $1025^\circ\text{C}$  under vacuum. Similar spreading kinetics were observed on the polished, dense type A material despite the presence of 1–2 wt% C in this material. This material had a terminal contact angle of  $9\text{--}12^\circ$  as measured on a smooth surface. Evidence for triple line pinning is seen in the shape of the thin spreading film that forms on these materials. The true wetting behavior of the type C & D materials was not revealed by the contact angle measurements. The 28.5% apparent porosity of the type C  $\text{TiB}_2$  resulted in substrate penetration that affected the contact angle measurement. Strong reaction between Al and the 5.5 wt% Ni of the type D  $\text{TiB}_2$  overcame the oxide film effects, but resulted in an expansion of the substrate that also affected the measured contact angle.

2. Wetting kinetics are greatly accelerated under a cryolitic salt cover which has a high solubility for the oxides of Al, B and Ti. The rate of spreading was much lower for samples held in 1 atm argon in a Zr crucible. This and published studies of the kinetics of the high-temperature alteration of surface oxides on  $\text{TiB}_2$  illustrate the effect they have on wetting kinetics. While

it was possible to reduce the oxygen content of the 1 atm hydrogen gas atmosphere low enough to prevent B<sub>2</sub>O<sub>3</sub> formation on TiB<sub>2</sub>, the rapid formation of an aluminum oxide layer on the Al sessile drop restrained drop spreading yielding artificially high contact angles. When the temperature was raised above 1300°C, approaching the B/B<sub>2</sub>O<sub>3</sub> equilibrium pO<sub>2</sub>, the rapid spreading behavior expected for the dense, high-purity TiB<sub>2</sub> was observed. In vacuum experiments a spreading stage was realized after hold times that coincide with the disappearance of B<sub>2</sub>O<sub>3</sub> from the surface.

3. A more thorough characterization of the oxide layers that form on a given TiB<sub>2</sub> substrate material under the exact conditions of the sessile drop wetting experiment is required to properly interpret the spreading behavior in systems prone to oxidation.

**Acknowledgements**

The management of Alcoa is acknowledged for its support of this work. Initial wetting studies were supported under DOE Cooperative Agreement No. DE-FCO7-98ID13666. Characterization of materials was conducted at both the University of Missouri at Rolla and the Alcoa Technical Center. The expertise of these analysts is recognized and appreciated.

**References**

1. H. ZHANG, V. DE NORA and J. A. SEKHAR, Materials used in the Hall-Heroult Cell for Aluminum Production, TMS, Warrendale, PA (1994) p. 108.
2. N. EUSTATHOPOULOS, M. G. NICHOLAS and B. DREVET, "Wettability at High Temperatures" (Pergamon, Amsterdam, 1999) p. 420.
3. S. K. RHEE, *J. Am. Ceram. Soc.* **53**(7) (1970) 386.
4. J. G. LI, *Ceram. Intern.* **20** (1994) 391.
5. G. V. SAMSONOV, A. D. PANASYUK and M. S. BOROVIKOVA, *Por. Metall.* **5**(125) (1973) 61.
6. N. EUSTATHOPOULOS and L. COUDURIER, *Ann. Chim. Fr. (Paris)* **10**(1) (1985) 1.
7. D. A. WEIRAUCH, JR., W. M. BALABA and A. J. PERROTTA, *J. Mater. Res.* **10**(3) (1995) 640.

8. A. BARDAL, K. NORD-VARHAUG, J. H. ULVENSOEN and E. SKYBAKMOEN, in Proc. 1st Int. Conf. On High-Temperature Capillarity, edited by N. Eustathopoulos (Bratislava, Slovakia, 1994) p. 93.
9. S. V. DEVYATKIN and G. KAPTAY, *J. Solid State Chem.* **154** (2000) 107.
10. C. MROZ, *Bull. Amer. Ceram. Soc.* **79**(6) (2000) 55.
11. H. R. BAUMGARTNER and R. A. STEIGER, *J. Amer. Ceram. Soc.* **67**(3) (1984) 207.
12. P. D. OWNBY, K. W. LI and D. A. WEIRAUCH, JR., *ibid.* **74**(6) (1991) 1275.
13. D. A. WEIRAUCH, JR., in Ceramic Microstructures'86, Role of Interfaces, Materials Science Research, Vol. 21, edited by J. A. Pask and A. G. Evans (Plenum Press, NY, 1988) p. 329.
14. D. A. WEIRAUCH, JR. and W. J. KRAFICK, *Metall. Trans. A* **21A** (1990) 1745.
15. H. JOHN and H. HAUSNER, *Int. J. High Tech. Ceram.* **2** (1986)73.
16. D. A. WEIRAUCH, JR., in "9th Int. Conf. High Temp. Materials," edited by K. E. Spear, Electrochem Soc. Proc., Vol. 97-39 (1997) p. 421.
17. K. GRJOTHEIM, C. KROHN, M. MALINOVSKY, K. MATIASOVSKY and J. THONSTAD, "Aluminum Electrolysis," 2nd. ed. (Aluminium-Verlag, Dusseldorf, 1982) p. 433.
18. C. B. FINCH and V. J. TENNERY, *J. Am. Ceram. Soc.* **65**(7) (1982) C100.
19. D. A. WEIRAUCH, JR. and W. J. KRAFICK, *J. Mater. Res.* **11**(8) (1996) 1897.
20. E. SAIZ, A. P. TOMSIA and R. M. CANNON, *Acta Mater.* **47**(7) (1998) 2349.
21. X. G. WANG, *J. Central-South Inst. Min. Metall.* **24**(5) (1993) 602.
22. K. LANDRY and N. EUSTATHOPOULOS, *Acta Mater.* **44**(10) (1996) 3923.
23. Y.-H. KOH, S.-Y. LEE and H.-E. KIM, *J. Am. Ceram. Soc.* **84**(1) (2001) 239.
24. K. D. WATSON and J. M. TOGURI, *Met. Trans.* **22B** (1991) 617.
25. JU V. NAIDICH, *Prog. Surf. Membr. Sci.* **14** (1981) 353.
26. E. A. BRANDES and G. B. BROOK (eds.), "Smithells Metals Reference Book" (Butterworth Heinemann, Oxford, UK) p. 14-6.
27. E. W. DEWING and P. DESCLAUX, *Met. Trans.* **8B** (1977) 555.

Received 31 March  
and accepted 20 October 2004